علـوم محـیـطی سال ششم، شماره چهارم، تابستان ۱۳۸۸
ENVIRONMENTAL SCIENCES Vol.6, No.4, Summer 2009
171-182

# Application of High Resolution Satellite Images for Large-Scale Map Revision Case Study: IKONOS Image of Urumia

**Ali Akbar Matkan[1*], Mohammad Sohrabinia[1], Saeid Sadeghian[2], Dadfar Manavi[3]**

*1- Department of Remote Sensing and GIS, Faculty of Earth Sciences, Shahid Beheshti University, G.C.*
*2- Geomatics College, National Cartographic Center (NCC), Tehran, Iran.*
*3- National Cartographic Center (NCC), Tehran, Iran.*

**Abstract**

In this study, we have analyzed how to update large scale maps with the help of IKONOS images. To do this, a complete frame IKONOS image from aerial photos (1:5000 scale) and 1:2000 scale digital maps of the city of Urumia have been used as test data. Here, our objective is to exploit the spatial precision of a pan-chromatic band, the spectral richness of a multispectral image and the spatial and spectral capabilities of a pan-sharpened product at the same time. Meanwhile, geometric correction, image fusion, image information extraction, change detection and incorporation of the changes into the old maps are the main subjects of discussion in the current research. At first, geometric correction of IKONOS image has been analyzed with the help of polynomial, rational and RPC functions, with tables and charts used to compare statistical results of these three models. Overall, the rational model with a third coefficient gave the best result. Geometric correction with the RPC model without any control points gave an RMS error of 15 meters, which decreased to 70 cm. when only one control point was applied. The model with the best results was used to produce ortho-images of IKONOS pan-chromatic and multispectral images. To extract different object classes from the IKONOS image, visual interpretation, pixel-based and fuzzy object extraction methods have been used. Aerial photographs and old maps were used for editing and accuracy assessment of the results. Image analysis methods for visual interpretation, training samples for supervised and fuzzy classification and interpretation of the output classes of unsupervised classification all proved to be very helpful. Further, to detect occurrences of changes occurred relative to the old maps, comparison of the old maps with new extracted maps and comparison of the old maps with the IKONOS image were carried out. Finally, the information content of the IKONOS image was compared with object classes of 1:5000 and 1:2000 scale maps. For 1:5000 scale maps, most of object classes were detectable and recognizable, however, only a limited number of classes in 1:2000 scale maps were detectable and recognizable. In sum, it was found that IKONOS images are capable for the revision of 1:5000 scale maps but has some deficiencies in 1:2000 scale maps.

*Keywords*: mathematical modeling, geometric correction, object extraction, information content, revision

## کاربردهای تصاویر ماهواره‌ای با توان تفکیک بالا در به هنگام سازی نقشه‌های بزرگ مقیاس مطالعه موردی : تصویر آیکونوس ارومیه

**علی اکبر متکان[1*]، محمد سهرابی‌نیا[1]، سعید صادقیان[2]، دادفر معنوی[3]**

*۱- گروه سنجش از دور و GIS، دانشکده علوم زمین، دانشگاه شهید بهشتی*
*۲- آموزشکده نقشه برداری، سازمان نقشه برداری کشور*
*۳- سازمان نقشه برداری کشور*

**چکیده**

در این تحقیق چگونگی به‌هنگام‌سازی نقشه‌های بزرگ مقیاس با استفاده از تصاویر سنجنده آیکونوس (IKONOS) مطرح می گردد. یک فریم کامل تصویر سنجنده مذکور که بخش بزرگی از شهر ارومیه را پوشش می‌دهد به همراه عکس‌های هوایی (مقیاس ۱:۵۰۰۰) و نقشه‌های رقومی (۱:۲۰۰۰) همان منطقه به عنوان داده‌های ورودی مورد استفاده قرار گرفته است. هدف اصلی ما بهره‌گیری از قابلیت‌های دقیق مکانی باند پانکروماتیک، طیفی باندهای چند طیفی و کارایی طیفی-مکانی این دو به طور همزمان در تصویر ترکیبی است. در همین راستا تصحیح هندسی، ادغام تصاویر، استخراج محتوی اطلاعاتی تصاویر، تشخیص تغییرات و بالاخره اعمال تغییرات استخراج شده در نقشه‌های موجود مباحث عمده این تحقیق هستند. تصحیح هندسی تصاویر با کمک مدل‌های پلی‌نومیال، رشنال و توابع RPC مورد تحلیل قرار گرفته است. در بخش مذکور مدل رشنال با ضریب سوم بهترین نتیجه را ارائه داده است. نکته قابل توجهی که در بکارگیری مدل RPC مشاهده گردید این بوده است که بدون بکارگیری نقاط کنترل زمینی دقت این مدل با ۱۵ متر خطا همراه بود، ولی با بکارگیری تنها یک نقطه کنترل این مقدار خطا به ۷۰ سانتیمتر کاهش یافت. نهایتا مدلی که بهترین نتایج را ارائه داده بود برای تولید تصاویر تصحیح شده پانکروماتیک و چند طیفی بکار گرفته شد. در بخش استخراج اطلاعات از تصاویر روش‌های تفسیر چشمی، پیکسل-مبنا و فازی مورد استفاده قرار گرفتند. ویرایش و بررسی دقت اطلاعات استخراج شده با کمک عکس‌های هوایی و نقشه‌های رقومی موجود به انجام رسید. برای روش تفسیر چشمی تحلیل تصاویر و در روش‌های طبقه‌بندی نظارت شده و فازی نمونه‌های آموزشی کارایی مفیدی داشتند. نمونه‌های آموزشی برای تفسیر و نامگذاری کلاس‌های طبقه‌بندی نظارت نشده نیز کمک موثری ایفا کردند. برای مرحله تشخیص تغییرات از دو روش مقایسه نقشه‌های موجود با اطلاعات وکتوری استخراج شده و مطابقت نقشه‌های موجود با تصویر آیکونوس کمک گرفته شد. در مرحله آخر محتوی اطلاعاتی تصاویر آیکونوس با طبقات عوارض موجود در نقشه‌های ۱:۲۰۰۰ و ۱:۵۰۰۰ مقابله گردید. اغلب طبقات عوارض نقشه‌های ۱:۵۰۰۰ و گروه محدودی از عوارض نقشه‌های ۱:۲۰۰۰ با کمک محتوی اطلاعاتی تصاویر آیکونوس قابل تشخیص و شناسایی بودند. بنابراین نتیجه گرفته شد که تصاویر آیکونوس برای به‌هنگام‌سازی نقشه‌های ۱:۵۰۰۰ مناسب ولی برای نقشه‌های ۱:۲۰۰۰ مواجه با نارسایی عمده می‌باشند.

*واژگان کلیدی:* مدلسازی ریاضی، تصحیح هندسی، استخراج عوارض، محتوی اطلاعاتی، بازنگری نقشه.

* Corresponding author. *E-mail Address:* A-matkan@sbu.ac.ir

## Introduction

Satellite remote sensing with its advent in the second half of the twentieth century has played a key role in monitoring and mapping the Earth's surface. Adequate data in short time intervals has been available from different parts of the Earth. Developments in satellite data collection technologies had been concordant with growth of applications of remote sensing data. Initiation of high resolution satellite sensors is one of those outstanding developments which have heralded new applications of remote sensing data, one of which is large scale mapping. IKONOS launched by Space Imaging[1] in September 1999 (Space Imaging, 2006) is the first commercial satellite which took images with a one-meter pixel size. QuickBird (2001), EROS A1 (2000) and a number of other satellites have followed it which have taken images about the same pixel sizes.

Maps are date stamped evidence of a locality preserving the state of Earth's surface in their production time. Maps are collected in different scales regarding to the spatial size of the objects to be registered on the maps and the extent of the area of interest. The larger the extent of the area to be displayed on a map, the smaller the size of the objects can be depicted and vice versa. Small scale maps cover vast areas such as a province, a whole country or even a continent on a single sheet. Large scale maps, on the other hand, are produced for specific purposes with a detailed information content of the area of interest. Large scale maps are mostly used in urban studies for different purposes. Urban land use, cadastre maps and digital land information databases about real estate ownership and utilities where exact awareness about boundaries of adjacent land parcels is required are prepared in larger scales. Revision and updating of these maps require accurate data with sufficient spatial precision. Before the introduction of high resolution sensors, the only source for updating these maps was aerial photography or land surveying which is costly and time consuming. With the help of new high resolution satellite images, updating of large scale maps has been improved.

Literally, in a map revision process, old maps and recent images are overlaid and compared in order to make changes recognizable. Using different information extraction methods from satellite images, the changed parts in maps are detected and modified. In this work, we analyze geometric correction, information extraction and different map revision methods in order to update large scale maps.

## Literature Review

The application of satellite images for the production and revision of large scale maps has been extensively analyzed by researchers around the world. Some of these works which have been used in current study are below summarized.

Patynen (1998) has described the revision process for the 1:5000, 1:10000 and 1:20000 scale Finish Topographic DataBase (TDB) using digital methods. He has noted that time intervals to update 1:20000 maps had been specified over 10-20 years but, in populated areas where changes are more rapid, this has been reduced to 5-10 years. He has outlined that some major facilities like roads, power lines and administrative structures need continuous updating (annually). He has explained the whole process of scanning, geometric registration and otho-photo creation and object extraction methods for TDB updating process. Fiset *et al.* (1998) studied the revision of 1:50000 scale maps with the help of SPOT-HRV satellite images. They compared maps and recent images to detect changes. Old topography and maps of the study area were used for the accuracy assessment. They used a method called Multi Layer Perception (MLP) for the comparison of the maps and different layers of the processed images. In this method, different layers of maps and images with different levels of processing are overlaid by optical devices.

Metternicht (1999) analyzed the revision of topographic maps with the help of remote sensing data and automatic image object extraction methods. He divided change detection in satellite images and aerial photographs into the two steps of before and after the

classification process. Division, image ratio and PCA are specified as the pre-classification steps, while comparison of the old maps and recent images were categorized as post-classification methods of image information extraction. After listing deficiencies of the above methods, he explores a methodology for computing changes using fuzzy modeling. Using fuzzy sets and fuzzy logic, likelihood of changes detected from remotely sensed images are defined.

Yi-jin and Xiao-wen (2004) have presented satellite image analysis for map revision. They have underlined the utilization of knowledge derived from existing GIS database as a priori knowledge in the image classification process. They have used cartographic semantics to extract objects from images based on geometry and topology rules. By identifying the differences between the image and the vector map, new geographic features and the changed features are detected. Depending on the results, the map is updated. Manavi studied the revision of 1:50000 scale maps with the help of IRS-1D images in Kerman, Iran. First, he tried to achieve sub-pixel accuracy in geometric correction of the IRS images. Then, he used three object extraction methods including automatic classification, visual interpretation and field check to detect object classes in 1:50000 scale maps. In his study, Manavi (2004) exploited spatial factors like the elevation, slope and pattern of the objects in the visual interpretation method to detect and recognize objects.

## Test Data and Study Area

Our data included an IKONOS image frame with four multispectral bands and a panchromatic band, aerial photographs of the same area with the scale of 1:5000 and digital maps with the scales of 1:10000, 1:5000 and 1:2000 also from the same area. The study area is covered by an IKONOS image frame of the northwestern Iranian city of Urumia. The coordinates of the image are: NW: 45-00-05 lon., 37-36-12 lat.; SE: 45-07-17 lon., 37 - 31 - 17 lat.

The image covers most of Urumia city (Figure 1). The northern and eastern parts of the image show the

**Figure1.** The study area image and distribution of GCPs (dark points) and ICPs (light points).

agricultural city margins with spotted industrial and other buildings. There are no conspicuous geographical phenomena in the image, and the terrain is relatively flat. There are only some low altitude hills on the top west margins of the image. The elevation ranges from 1300 meters in low level drainage basins to 1430 meters at the western hills. As most parts of the image have elevations around 1310 to 1350 meters which demonstrates that the terrain is relatively flat.

## Geometric Correction Methods

In order for imagery to be utilized in GIS and other applications for which pixels must be correctly geo-located, image ortho-rectification is a necessity (Mercer *et al.*, 2003). Therefore, three geometric correction methods were analyzed and the results were compared to find the model with the best accuracy. These are the polynomial, rational and RPC models. For all the models, different combinations of GCP[2]s and ICP[3]s were used (Table 1). Combinations 1 to 14 were used in all three models but the last three combinations only were used for the RPC model. The results of the models were compared to find the most accurate one in order to be used in ortho-rectification of the images.

## Polynomial Model

The polynomial model in its first order is a simple linear mathematical function with three unknown parameters. This model posseses five orders extending from one to five. Different combinations of GCP and ICPs have been used for different orders of the polynomial model (Table 1). Accuracies of each combination for each order of the model listed in a table. Charts of these tables were prepared for better analysis and comparison of the results. The third order of the model gave the best overall result, where the amounts of RMS error for the ICPs are the lowest among other orders (Table 2). As can be understood from its name, ICPs are calculated independently from the model; therefore, its accuracy is more reliable. RMS errors in this order are less than a half of the pixel size of the study image (Figure 2).

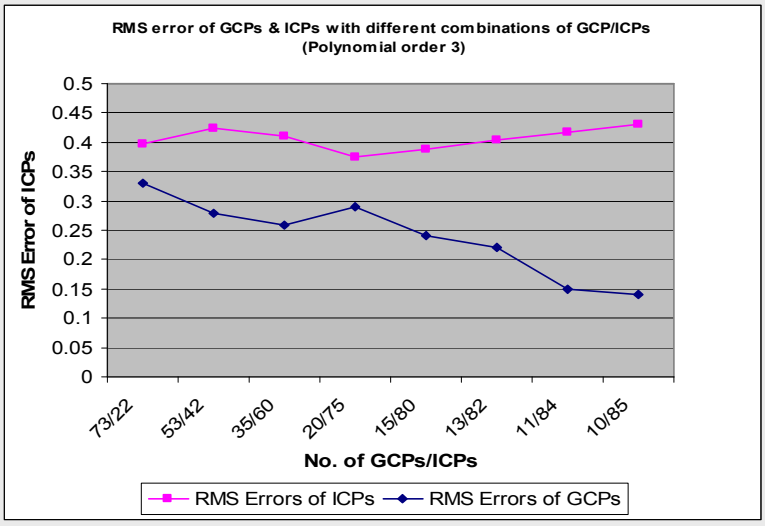


**Figure 1.** Accuracies of third order of polynomial model (accuracies are in meters).

## Rational Function Model (RFM)

An image coordinate is determined from a ratio of two polynomial functions (ITL, 2006):

(1)

$$r = P1(X,Y,Z) / P2(X,Y,Z) = \sum_{i=0}^{m1}\sum_{j=0}^{m2}\sum_{k=0}^{m3} a_{ijk} X^i Y^J Z^k \Big/ \sum_{i=0}^{n1}\sum_{j=0}^{n2}\sum_{k=0}^{n3} b_{ijk} X^i Y^J Z^k$$

$$c = P3(X,Y,Z) / P4(X,Y,Z) = \sum_{i=0}^{m1}\sum_{j=0}^{m2}\sum_{k=0}^{m3} c_{ijk} X^i Y^J Z^k \Big/ \sum_{i=0}^{n1}\sum_{j=0}^{n2}\sum_{k=0}^{n3} d_{ijk} X^i Y^J Z^k$$

Where r and c are normalized pixel coordinates on the image; X,Y,Z are normalized 3D coordinates on the ground (map and DEM); $a_{ijk}$, $b_{ijk}$, $c_{ijk}$, $d_{ijk}$ are polynomial coefficients. The RFM maps three-dimensional ground coordinates to image space on all types of sensors such as frame, pushbroom, whiskbroom and SAR systems.

Rational functions have 18 coefficients starting from 3 and extending to 20. Different combinations of GCPs/ICPs have been used to calculate accuracies for the coefficients of this model. The amounts of RMS errors are listed in a table to analyze and compare the results (Table 3). Maximum accuracy has been achieved in the third coefficient (which is the first coefficient of this model). RMS errors in this coefficient are less than a half of the pixel size of IKONOS panchromatic image (Figure 3).

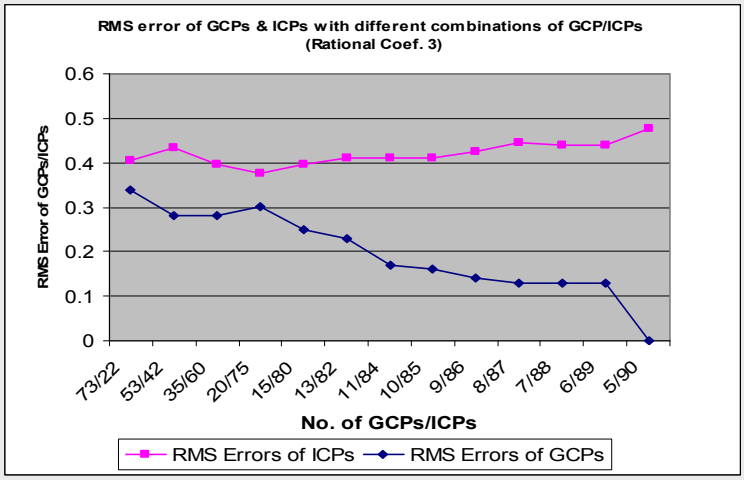


**Figure 3.** Accuracies of third coefficient of rational model (m)

**Table 1.** Different GCP/ICP combinations used for mathematical modeling.

| Combinations / Points | 1 | 2 | 3 | 4 | 5 | 6 | 7 | 8 | 9 | 10 | 11 | 12 | 13 | 14 | 15 | 16 | 17 |
|---|---|---|---|---|---|---|---|---|---|---|---|---|---|---|---|---|---|
| GCPs | 73 | 53 | 35 | 20 | 15 | 13 | 11 | 10 | 9 | 8 | 7 | 6 | 5 | 4 | 3 | 2 | 1 |
| ICPs | 22 | 42 | 60 | 75 | 80 | 82 | 84 | 85 | 86 | 87 | 88 | 89 | 90 | 91 | 92 | 93 | 94 |

**Table 2.** Results of the Polynomial model for the first combination of GCP/ICPs (m).

| Orders | GCPs: 73 | | | ICPs: 22 | | |
|---|---|---|---|---|---|---|
| | dx | Dy | dxy | dx | dy | dxy |
| 1 | 0.25 | 0.25 | 0.35 | 0.3 | 0.28 | 0.410366 |
| 2 | 0.24 | 0.23 | 0.33 | 0.3 | 0.27 | 0.403609 |
| 3 | 0.24 | 0.24 | 0.33 | 0.3 | 0.26 | 0.396989 |
| 4 | 0.24 | 0.23 | 0.33 | 0.3 | 0.27 | 0.403609 |
| 5 | 0.24 | 0.23 | 0.33 | 0.3 | 0.27 | 0.403609 |

**Table 3.** Results of the rational model for the first combination of GCPs/ICPs (m).

| Coefficients | GCPs: 73 | | | ICPs: 22 | | |
|---|---|---|---|---|---|---|
| | dx | Dy | dxy | dx | dy | Dxy |
| **3** | 0.24 | 0.24 | 0.34 | 0.31 | 0.26 | 0.4046 |
| **4** | 0.23 | 0.23 | 0.33 | 0.32 | 0.29 | 0.4319 |
| **5** | 0.23 | 0.23 | 0.32 | 0.31 | 0.29 | 0.4245 |
| **6** | 0.23 | 0.22 | 0.32 | 0.31 | 0.29 | 0.4245 |
| **7** | 0.23 | 0.22 | 0.32 | 0.29 | 0.3 | 0.4173 |
| **8** | 0.23 | 0.22 | 0.32 | 0.29 | 0.31 | 0.4245 |
| **9** | 0.22 | 0.22 | 0.31 | 0.29 | 0.31 | 0.4245 |
| **10** | 0.22 | 0.22 | 0.31 | 0.3 | 0.31 | 0.4314 |
| **11** | 0.22 | 0.22 | 0.31 | 0.3 | 0.33 | 0.4460 |
| **12** | 0.22 | 0.21 | 0.31 | 0.3 | 0.38 | 0.4841 |
| **13** | 0.22 | 0.22 | 0.31 | 0.3 | 0.36 | 0.4686 |
| **14** | 0.22 | 0.22 | 0.31 | 0.3 | 0.36 | 0.4686 |
| **15** | 0.22 | 0.21 | 0.3 | 0.28 | 0.4 | 0.4883 |
| **16** | 0.21 | 0.21 | 0.3 | 0.32 | 0.4 | 0.5122 |
| **17** | 0.21 | 0.21 | 0.3 | 0.32 | 0.4 | 0.5122 |
| **18** | 0.21 | 0.21 | 0.3 | 0.32 | 0.46 | 0.5604 |
| **19** | 0.21 | 0.21 | 0.3 | 0.31 | 0.46 | 0.5547 |
| **20** | 0.21 | 0.21 | 0.3 | 0.31 | 0.46 | 0.5547 |

## RPC Model

The RPC model can be expressed simply as a ratio of two cubic polynomials (ITL, 2006). The equation 1 can be rewritten as follows (Hu et al., 2004):

$$r = (1\ Z\ Y\ X \dots Y^3\ X^3).(a_0\ a_1 \dots a_{19})^T / (1\ Z\ Y\ X \dots Y^3\ X^3).(1\ b_1 \dots b_{19})^T \quad (2)$$

$$c = (1\ Z\ Y\ X \dots Y^3\ X^3).(c_0\ c_1 \dots c_{19})^T / (1\ Z\ Y\ X \dots Y^3\ X^3).(1\ d_1 \dots d_{19})^T$$

A least-squares approach can be utilized to determine the RPC model coefficients $a_i$, $b_i$, $c_i$ and $d_i$ from a 3-dimensional grid of points generated by intersecting the rays emanating from a 2-d grid of image points – computed using the physical camera model – with a number of constant elevation planes.

For the previous models, only the first 14 combinations of GCPs/ICPs were used while in the RPC model all of the combinations presented in Table 1 used to estimate the accuracies of the model. The RPC model can be calculated without any GCPs, but with a higher RMS error. Without using any GCPs the model resulted in a 15 meter RMS error whereas, using only one GCP, this amount was reduced to 70 cm. Best results (for check points) were achieved when only 10 control points and 80 check points were used (Table 4). When only one control point is used, the RMS error was still less than the pixel size of the image (Figure 4). The milestone of the RPC model is that we can achieve a satisfactory accuracy using the least number of control points. This will result in less cost for the collection of control points, especially where the study area falls in an area that we have some natural or political constraints in terms of access to GCP collection.

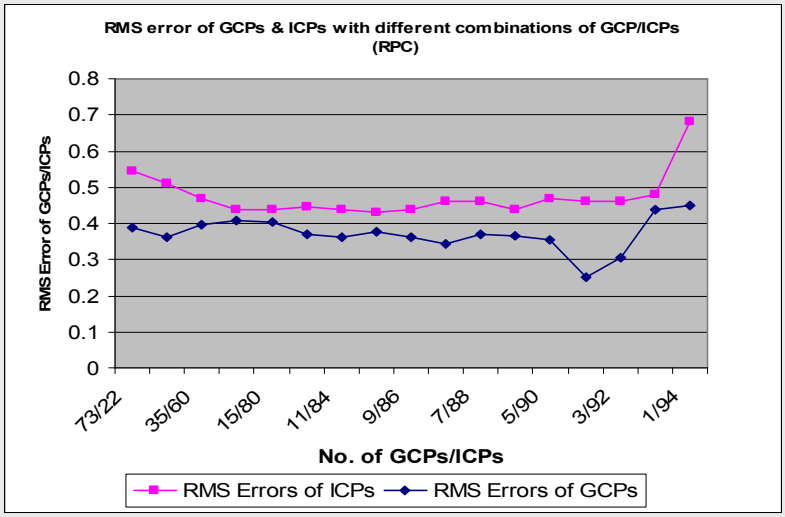


**Figure 4.** Accuracies of RPC model (m).

**Table 4.** Accuracies of the RPC model in all combinations of GCPs/ICPs (m).

| GCPs/ICPs | GCPs | | | ICPs | | |
|---|---|---|---|---|---|---|
| | dx | dy | dxy | dx | dy | dxy |
| **73/22** | 0.28 | 0.27 | 0.388973 | 0.4 | 0.37 | 0.544885 |
| **53/42** | 0.25 | 0.26 | 0.360694 | 0.38 | 0.34 | 0.509902 |
| **35/60** | 0.28 | 0.28 | 0.39598 | 0.33 | 0.33 | 0.46669 |
| **20/75** | 0.24 | 0.33 | 0.408044 | 0.33 | 0.29 | 0.439318 |
| **15/80** | 0.23 | 0.33 | 0.402244 | 0.33 | 0.29 | 0.439318 |
| **13/82** | 0.24 | 0.28 | 0.368782 | 0.33 | 0.3 | 0.445982 |
| **11/84** | 0.23 | 0.28 | 0.362353 | 0.32 | 0.3 | 0.438634 |
| **10/85** | 0.24 | 0.29 | 0.376431 | 0.32 | 0.29 | 0.431856 |
| **9/86** | 0.25 | 0.26 | 0.360694 | 0.32 | 0.3 | 0.438634 |
| **8/87** | 0.21 | 0.27 | 0.342053 | 0.34 | 0.31 | 0.460109 |
| **7/88** | 0.23 | 0.29 | 0.370135 | 0.34 | 0.31 | 0.460109 |
| **6/89** | 0.21 | 0.3 | 0.366197 | 0.32 | 0.3 | 0.438634 |
| **5/90** | 0.13 | 0.33 | 0.354683 | 0.35 | 0.31 | 0.467547 |
| **4/91** | 0.15 | 0.2 | 0.25 | 0.35 | 0.3 | 0.460977 |
| **3/92** | 0.19 | 0.24 | 0.306105 | 0.35 | 0.3 | 0.460977 |
| **2/93** | 0.25 | 0.36 | 0.438292 | 0.34 | 0.34 | 0.480833 |
| **1/94** | 0.28 | 0.35 | 0.448219 | 0.36 | 0.58 | 0.682642 |

**Comparison of the Results of Mathematical Models**

After analyzing three mathematical models, we used the best result of these models to find the model with better accuracy to produce the final ortho-image. As mentioned above, polynomial order 3 and rational coefficient 3 had better accuracies compared with other orders and coefficients of the models. These are used to draw a chart, together with the accuracies of the RPC model to find the best model (Figure 5). In this comparison chart, we see that the best accuracies are achieved with Rational Coefficient-3 for ICPs and Polynomial Order-3 for GCPs. The worst accuracies for both GCPs and ICPs are achieved with the RPC model. Since the ICPs are calculated independently from the model, they are more reliable; we therefore used the Rational Coefficient-3 as the most accurate model to produce the ortho-image of the study area.

## Ortho- Image of the Study Area

As the rational model with a third coefficient gave the best results for the mathematical modeling process, we used it to produce an ortho-image from the pan-chromatic band of the IKONOS image. At first, four multispectral bands of the image had separately undergone a geometrical correction process using the RPC files of each band. Then, a multispectral image using all four bands of the image were produced. Using the Rational Coefficient-3, this image also used to produce a multispecral ortho-image. Until now, we only had ortho-images of the panchromatic band with a pixel size of one meter and a multispectral image with a pixel size of four meters. To produce a pan-sharpened product using these two images, different image fusion methods were analyzed. The PCA[4] method with respect to its better spatial accuracy was chosen to produce the pan-sharpened product.

## Object Extraction Methods

Three object extraction methods were applied to extract object classes from the IKONOS image, namely visual interpretation, image classification and fuzzy object extraction.

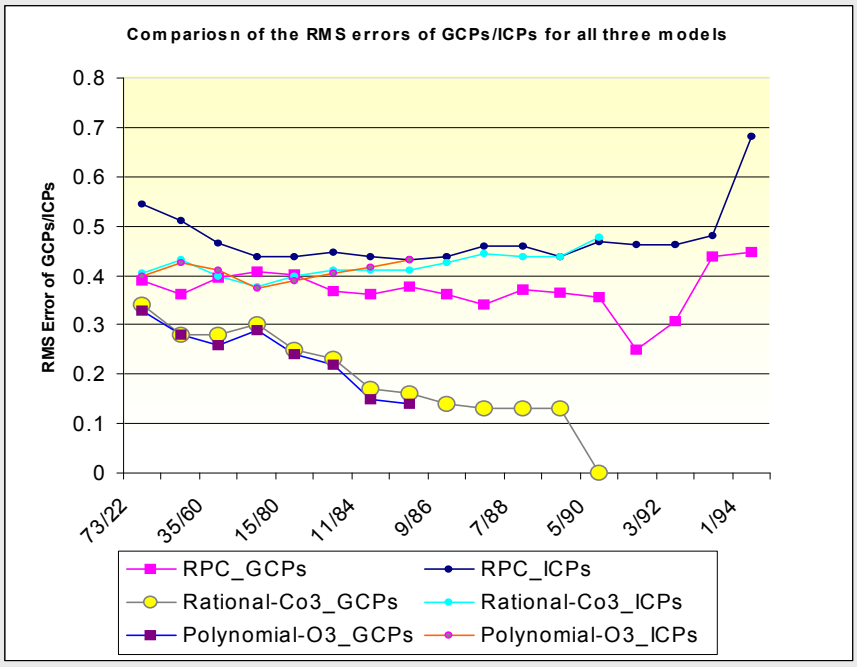


**Figure 5.** Comparison of the accuracies in meters for all three models, polynomial order-3, rational coefficient-3 and RPC.

For the visual interpretation, different image analysis methods were used to better extract object classes. In the automatic classification method, supervised and unsupervised methods were used to classify object classes. Training samples were extracted from the image with the help of aerial photographs and digital maps to be used in unsupervised classification. These training samples were also used for the fuzzy classification, which was implemented by eCognition and IDRISI softwares. All of the information extracted from visual interpretation, automatic classification and fuzzy methods was converted to vector layers. These vector layers then used to compare with the old maps in order to detect changes occurred relative to the old maps.

## Change Detection

After creating the ortho-image, we overlaid vector maps on the image. Both new extracted vector layers and the old maps were used in the overlay process to compare the old maps with the new extracted vector layers and the IKONOS image. Old vector maps have a 1:2000 scale, so not all of their features can be extracted from IKONOS images. As mentioned before, the image was acquired on March 2006 and the maps were extracted from aerial photographs and ground surveying from 2002, i.e. about four years of difference. We analyzed the image and the vector maps to find those parts in the image that has been changed since 2002. In some parts, changes were obvious, for example a new building has been constructed (Figure 7) or a road expanded. But in some other parts like agricultural fields, changes are not so distinct, where the source of change is related to different kinds of crops cultivated each year. While a city expands, fields become deserted and converted to roads or other constructions (Figure 6).

We checked the feature classes contained in 1:10000, 1:5000 and 1:2000 scale maps in the study image. These feature class lists are prepared by the NCC (National Cartographic Center) of Iran based on cartographic standards and experience built up over years of mapping missions. Most of information content for smaller scales were detected and recognized but little information content in 1:2000 maps was detectable. Some feature classes, such as small buildings and even cars, which are detectable cannot be recognized. We could hardly specify exact bounds of these smaller buildings for 1:2000 scale maps and there were mixed pixels in margins. Of

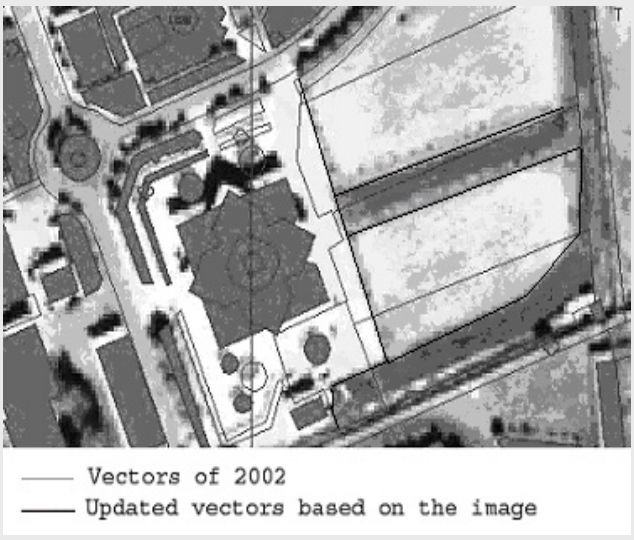


**Figure 6.** Borders of fields have changed and new street is constructed since 2002. Also it seems fields have been deserted.

**Figure 7.** New buildings constructed since 2002.

course, in these cases, the accuracy is acceptable for the larger scales of 1:5000 and 1:10000. We analyzed our results and compared them with other work carried out previously. All groups of features in 1:10000 are detectable; most groups of 1:5000 scale maps and only a little number of groups of features in 1:2000 scale maps are detectable in IKONOS images (Sadeghian *et al.*, 2001; Samadzadegan *et al.*, 2004). While our test area maps were 1:2000, only a few groups of features were detectable and could be updated. But larger phenomena like blocks of buildings and industrial constructions, agricultural fields, streets, road crossings were detectable.

## Conclusion

Based on the results of the geometric models, the best geometric correction model to rectify the IKONOS image of the study area is the rational model with a third coefficient. Since spatial resolution of IKONOS Geo Multispectral bands differs with panchromatic band, correcting them separately will give conflicting results. Geo level geometric corrections use RPC files for each of the image bands which are provided by the SI Company. These files are not dependent on the pixel size of the images and give equal accuracies for all bands of the image. Accordingly, individual pixels in each of the multispectral bands and the panchromatic band with Geo level correction would posses a complete compatibility. When a band combination or image fusion processes are applied to these bands, objects on each band will fit with the other bands and the final image will look quite natural. Therefore, it is better to run an image fusion process using panchromatic and multispectral images before conducting geometric corrections.

At the object extraction stage, training samples proved to be very helpful both in supervised as well as fuzzy image classification methods. Based on visual interpretation and using old maps, IKONOS image and aerial photographs, training samples were selected. Different processing levels of the IKONOS image (PCA image, Ratio images) were also helpful in selecting training sites.

The precision of geometric correction was a crucial factor in the change detection process, as well. Precise overlay and fitness of the objects both in the old maps and the new extracted vector layers on the IKONOS image was a key factor in the change detection process. Comparison of the new vector layers with the old maps had superiority in terms of

allowing the possibility of changing color and displaying different layers to make changes more conspicuous.


## Acknowledgement

The authors sincerely acknowledge National Cartographic Center of Iran for providing IKONOS image and 1:2000 scale 3D digital maps of the study area.


## Note

[1]- Space Imaging is a company based in US and founded in 1994 which is active in the fields of electronics and space. IKONOS is owned by this company.

[2]- Ground Control Points

[3]- Independent Check Points

[4] -Principal Components Analysis

## References


Fiset, R., F. Cavayas, M. C. Mouchot, B. Solaiman and R. Desjardins (1997). Map-image matching using a multi-layer perceptron: the case of the road network, *ISPRS. Journal of Photogrammetry & Remote Sensing*, 53**:** 76-84.

Floyd, F. and J. R. Sabins (1987). *Remote Sensing Principles and Interpretation.* Second Edition. New York: W. H. Freeman Company.

Hu, Y., V. Tao and A. Croitoru (2004). Understanding the Rational Function Model: Methods and Applications. *Proc. of the XXth International Society for Photogrammetry and Remote Sensing (ISPRS) Congress*, Istanbul.

Information Technology Laboratory (2006). Engineering statistics handbook. *http://www.itl.nist.gov/ div898/ handbook/pmd/section6/pmd642.htm.*

Jenson, J. R. (1996). *Introductory Digital Image Processing: A Remote Sensing Perspective.*New Jersey: Simon & Schuster.

Leica Geosystems (2003). *Erdas Field Guide*, Seventh Edition, GIS and Mapping. Atlanta: LLC.

Manavi, D. (2004). *Revision of 1:50000 scale maps of Iran with the help of IRS-1D satellite images, Case Study: 1:50000 scale map of Kerman.* Thesis for MSc. Degree, Department of Remote Sensing and GIS Faculty of Earth Sciences, Shahid Beheshti University.

Mercer, J. B., J. Allan, N. Glass., J. Rasmussen and M. Wollersheim (2003). Orthorectification of Satellite Images using External DEMs from IFSAR. *Proc. Joint ISPRS Workshop on High Resolution Mapping from Space*, Hannover, Germany, October $^{6\text{-}8}$th, Commission II, Working Group II/2.

Metternicht, G. (1999). Change detection assessment using fuzzy sets and remotely sensed data: an application of topographic map revision, *ISPRS. Journal of Photogrammetry & Remote Sensing*, 54: 221–233

Patynen, V. (1998). Digital orthophotos and map revision in National Land Survey of Finland. ISPRS Commission IV on GIS-Between Visions and Applications, Stuttgart, Germany. *IAPRS*, 32 (4).

Richards, J. A. (1993). *Remote Sensing Digital Image Processing: An Introduction.* Berlin: Springer-Verlag.

Sadeghian, S., M. J. Valadan Zoej, M. R. Delavar and A. Abootalebi (2001). Precision rectification of KFA-1000 and IKONOS images using the multiquadric and DLT model over test areas in IRAN. *Photogrammetric Journal of Finland,* 17 (2): 69-77.

Samadzadegan, F., M. Sarpulaki, A. Abootalebi and A. Talebzadeh (2003). Evaluation of the map revision potential of IKONOS satellite imageries,

*National Geomatics Symposium*,Tehran, National Cartographic Center (NCC).

Shorts, N. (2006). "Remote Sensing Tutorial". *http://rst.gsfc.nasa.gov/Sect1/Sect1_15.html*.

Space Imaging (2006). *http://www.spaceimaging.com/products/imagery.htm*.

Tortosa, D. (2006).Geoforum. *http://hosting.soonet.ca/eliris/ remotesensing/bl130lec10.html*.

Yi-jin, C. and L. Xiao-wen (2004). Cartographic Semantics and Remote Sensing Data for Map Revision. *IEEE International Geoscience and Remote Sensing Symposium proceedings*, 20-24 September, Anchorage, Alaska.